Symmetric Positive-Definite Cartesian Tensor Orientation Distribution Functions (CT-ODF)

Yonas T. Weldeselassie[1], Angelos Barmpoutis[2], and M. Stella Atkins[1]

[1] School of Computing Science, Simon Fraser University
[2] Dept. of Computer & Information Science and Engineering, University of Florida*

Abstract. A novel method for estimating a field of orientation distribution functions (ODF) from a given set of DW-MR images is presented. We model the ODF by Cartesian tensor basis using a parametrization that explicitly enforces the positive definite property to the computed ODF. The computed Cartesian tensors, dubbed Cartesian Tensor-ODF (CT-ODF), are symmetric positive definite tensors whose coefficients can be efficiently estimated by solving a linear system with non-negative constraints. Furthermore, we show how to use our method for converting higher-order diffusion tensors to CT-ODFs, which is an essential task since the maxima of higher-order tensors do not correspond to the underlying fiber orientations. We quantitatively evaluate our method using simulated DW-MR images as well as a real brain dataset from a post-mortem porcine brain. The results conclusively demonstrate the superiority of the proposed technique over several existing multi-fiber reconstruction methods.

1 Introduction

Diffusion tensor imaging (DT-MRI) is a non-invasive imaging technique that measures the self-diffusion of water molecules in the body, thus capturing the microstructure of the underlying tissues. Second order symmetric positive definite (SPD) tensors have commonly been used to model the diffusivity profile at each voxel with the assumption of a single coherent fiber tract per voxel. Under this assumption diffusivity was defined as $d(g) = g^T Dg$ where g is the diffusion weighting magnetic gradient vector and D is the 2^{nd} order tensor to be estimated from a set of DW-MR images. This model, despite its simplicity and robustness, has been shown to be incorrect in regions containing intra-voxel orientational heterogeneity such as crossing and merging of fiber bundles [1,2].

Several methods have been proposed to overcome the single fiber orientation limitation of second order tensors. Tuch et al. [1] proposed the use of diffusion imaging

* Implementation code of our method is available through Matlab Central. This work was partially funded by the Canadian Natural Sciences and Engineering Research Council (NSERC). We thank Dr. Tim Dyrby, Danish Research Centre for Magnetic Resonance, Copenhagen University Hospital, Hvidovre, Denmark, for providing the porcine dataset.

T. Jiang et al. (Eds.): MICCAI 2010, Part I, LNCS 6361, pp. 582–589, 2010.

with diffusion weighting gradients applied along many directions distributed almost isotropically on the surface of a unit sphere; a method known as high angular resolution diffusion imaging (HARDI). In contrast to rank 2 tensors, this method does not assume any a priori knowledge about the diffusivity profile. A number of approaches have been proposed to compute the ensemble-average diffusion propagator P(r, t) of HARDI data. These methods include q-ball imaging (QBI) [3], diffusion spectrum imaging (DSI) [4], and diffusion orientation transform (DOT) [5]. These methods, collectively known as q-space imaging techniques, identify multiple fibers components by calculating the probability distribution function (PDF) of the diffusion process in each voxel, based on the Fourier transform relationship between the PDF of diffusion displacement and the diffusion weighted signal attenuation in q-space. DSI performs a discrete Fourier transform to obtain P(r,t), which requires a time intensive Cartesian sampling in q-space and hence is impractical for routine clinical use. QBI method takes measurements on a q-space ball and approximates the radial integral of the displacement probability distribution function by the spherical Funk-Radon transform. One problem with QBI is that the estimated diffusion orientation distribution function(ODF) is modulated by a zeroth-order Bessel function that induces spectral broadening of the diffusion peaks. DOT computes ODF at a fixed radius by expressing the Fourier transform in spherical coordinates and evaluating the radial part of the integral analytically assuming signals decay can be described by either a mono or a multi-exponential model, where the latter requires data acquisition over multiple concentric spheres, a time consuming proposition.

Another approach for multi-fiber reconstruction is to describe the apparent diffusion coefficient (ADC) by higher order diffusion tensors (e.g. 4^{th} and 6^{th}) that generalize the 2^{nd} order tensors and have the ability to approximate multi-lobed functions [6]. Several methods have been proposed for estimating 4^{th} order tensors with positive definite constraints [7,8,9] as well as for processing higher order tensor fields [10]. This approach is attractive not only because the rich set of processing and analysis algorithms developed for second order tensor fields can be extended for higher order tensors but also unlike spherical harmonics basis, the local maxima of higher order tensors can be easily computed [11,12] due to their simple polynomial form. Unfortunately, the use of higher order diffusion tensors has been confined to the estimation of tensor ADC profiles, although it is now known that the local maxima of ADC profiles estimated using higher order tensors generally can not be used to directly represent the orientations for the intravoxel crossing fibers [2,13,14].

In this paper, we propose the use of higher order SPD Cartesian tensors to model ODF profiles and present a novel method for estimating tensor field of ODF profiles from a given set of Diffusion-Weighted MR images. In our technique the ODF is modeled by Cartesian tensor basis using a parametrization that explicitly enforces the positive definite property to the computed distribution functions. The computed Cartesian tensor ODFs (CT-ODFs) are SPD tensors whose coefficients can be efficiently estimated by solving a linear system with non-negative constraints.

We quantitatively evaluate our method and demonstrate the superiority of the proposed technique over several existing multi-fiber reconstruction methods.

There are two main contributions in this paper: 1) We present a novel method for positive-definite CT-ODF estimation from DW-MRI. To the best of our knowledge there is no existing ODF model in literature that imposes explicitly the positivity to the estimated ODF, which is naturally a positive-valued spherical function. 2) We present a use full application of our method for converting higher-order diffusion tensor ADC profiles to CT-ODFs. We should emphasize that this is an essential task since the maxima of higher-order tensors do not correspond to the underlying fiber orientations. On the other hand, our method computes Cartesian Tensor ODFs whose maxima can be computed analytically and correspond to the true axonal orientations.

2 Method

2.1 Symmetric Positive-Definite Cartesian Tensors of Even Orders

Any spherical function $f(\mathbf{g})$ can be approximated by higher order Cartesian tensors:

$$f(\mathbf{g}) = \sum_{i=1}^{3}\sum_{j=2}^{3}\cdots\sum_{l=1}^{3} g_i g_j \cdots g_l C_{i,j,\cdots,l} \tag{1}$$

where g_i is the $i-th$ component of the 3-dimensional unit vector $\mathbf{g}$, and $C_{i,j,\cdots,l}$ are the coefficients of the $l-th$ order tensor.

When approximating certain spherical functions in DW-MRI, we are interested in tensors of even orders with full symmetry, due to the antipodal symmetric nature of the DW-MR signal acquisition. In this case of symmetry, those tensor coefficients which correspond to the same monomial $g_1^a g_2^b g_3^c$ are equal to each other (e.g. $C_{2,2,2,1} = C_{2,2,1,2} = C_{2,1,2,2} = C_{1,2,2,2}$, since they all correspond to the monomial $g_1 g_2^3$).

Furthermore, if the approximated function $f(\mathbf{g})$ is a positive-valued function, the Cartesian tensor should be positive-definite, i.e. $f(\mathbf{g}) > 0 \; \forall \; \mathbf{g} \in S_2$. Therefore Eq. 1 needs to be re-parametrized such that this positivity property is adhered to. In this work, we use the higher-order positive-definite tensor parametrization that has been recently proposed in [9]. According to this parametrization, any non-negative spherical function can be written as a positive-definite L^{th} order homogeneous polynomial in 3 variables, which is expressed as a sum of squares of $(L/2)^{th}$ order homogeneous polynomials $p(g_1, g_2, g_3; \mathbf{c})$, where $\mathbf{c}$ is a vector that contains the polynomial coefficients.

$$f(\mathbf{g}) = \sum_{j=1}^{M} \lambda_j p(g_1, g_2, g_3; \mathbf{c}_j)^2 \tag{2}$$

The parameters λ_j in Eq. 2 are non-negative weights. This parametrization approximates the space of L^{th} order SPD tensors and the approximation accuracy depends on how well the set of vectors $\mathbf{c}_j$ sample the space of unit vectors $\mathbf{c}$. It has been shown that by constructing a large enough set of well sampled vectors $\mathbf{c}_j$, we can achieve any desired level of accuracy [9].

2.2 Positive-Definite Cartesian Tensor ODF (CT-ODF) Profiles

The Diffusion-Weighted MR signal for a given magnetic gradient orientation $\mathbf{g}$ and gradient weighting b, can be modeled using the standard multi-fiber reconstruction framework as follows

$$S(\mathbf{g}, b) = \int_{S_2} w(\mathbf{v}) B(\mathbf{v}, \mathbf{g}, b) d\mathbf{v} \tag{3}$$

where the integration is over all unit vectors $\mathbf{v}$, $B(\mathbf{v}, \mathbf{g}, b)$ is a basis function, and $w(\mathbf{v})$ is a non-negative spherical function that can be seen as a mixing/weighting function. There have been several proposed models for the basis function $B()$ such as a Rigaut-type function [15], von Mises-Fisher distribution [16] and others. In all of these models, the integral in Eq. 3 cannot be computed analytically, thus one needs to approximate the space of unit vectors $\mathbf{v}$ by a discrete set of vectors $\mathbf{v}_1, \cdots, \mathbf{v}_K$. In this case Eq. 3 is correctly discretized by $S(\mathbf{g}, b) = \sum_{k=1}^{K} w_k B(\mathbf{v}_k, \mathbf{g}, b)$ iff there are at most K underlying neural fibers that are oriented necessarily along the vectors $\mathbf{v}_k$. Another problem with the aforementioned discretization is that the function $w()$ is not anymore continuous over the sphere (it equals to w_k for $\mathbf{v}_k$ and it is zero everywhere else).

The main idea in this paper is to avoid the above unnatural discretization of the space of orientations, by using a blending function $w()$, which can be appropriately decomposed so that: 1) it is positive-definite, and 2) is continuous over the sphere. In this work, we model such blending function as a L^{th} order SPD tensor (say 4^{th}) by plugging Eq. 2 into Eq. 3 as follows

$$S(\mathbf{g}, b) = \int_{S_2} \sum_{j=1}^{M} \lambda_j p(v_1, v_2, v_3; \mathbf{c}_j)^2 B(\mathbf{v}, \mathbf{g}, b) d\mathbf{v} \tag{4}$$

where v_1, v_2, v_3 are the three components of the unit vector $\mathbf{v}$.

Given a data set of DW-MRI signal attenuations S_i/S_0 associated with magnetic gradient orientations g_i and diffusion weighting b-value b, the coefficients of a L^{th} order positive-definite CT-ODF can be estimated by minimizing the following energy function with respect to the unknown polynomial-weighting coefficients λ_j

$$E = \sum_{i=1}^{N} \Big(S_i/S_0 - \sum_{j=1}^{M} \lambda_j \int_{S_2} p(v_1, v_2, v_3; \mathbf{c}_j)^2 B(\mathbf{v}, \mathbf{g}_i, b) d\mathbf{v} \Big)^2 \tag{5}$$

In order for the basis function $B()$ to reflect the signal attenuation of a single and highly oriented fiber response, we require the basis function to be a Gaussian that represents the diffusion process which is highly restricted perpendicular to the orientation $\mathbf{v}$. This is given by

$$B(\mathbf{v}, \mathbf{g}, b) = \lim_{\delta \to +\infty} e^{-\delta (\mathbf{v}^T \mathbf{g})^2} \tag{6}$$

Here we should emphasize that the model in Eq. 6 agrees with the properties of the DW-MR signal response, i.e. it takes maximum and minimum values for

diffusion sensitizing gradient orientations $\mathbf{g}$ that are perpendicular and parallel to the underlying fiber orientation $\mathbf{v}$ respectively. Moreover, δ is such that it captures information about b and mean diffusivity (D) and can be adjusted by altering either b or D. So this 'symmetry' can be simplified by using only δ in Eq. 6.

In order to compute the CT-ODF, we need to solve Eq. 5 for $\lambda'_j s$. This problem can be rewritten into an equivalent linear system problem $\mathbf{Bx} = \mathbf{y}$ where $\mathbf{x}$ is an M-dimensional vector of the unknown λ_j, $\mathbf{y}$ is an N-dimensional vector containing the given signal attenuations S/S_i and $\mathbf{B}$ is a matrix of size $N \times M$ with the elements $\mathbf{B}_{i,j} = \int_{S_2} p(v_1, v_2, v_3; \mathbf{c}_j)^2 B(\mathbf{v}, \mathbf{g}_i, b) d\mathbf{v}$.

This linear system is solved for the non-negative $\mathbf{x}$ using the efficient non-negative least squares algorithm and runs in 12ms/voxel. We can then easily compute the CT-ODF coefficients by multiplying the solution vector with a matrix $\mathbf{C}$, (i.e. $\mathbf{Cx}$), where the matrix $\mathbf{C}$ is of size $\frac{(2+L)!}{2(L!)} \times M$ that contains monomials formed by the vectors $\mathbf{c}_j$. Note that L is the order of the CT-ODF and $\frac{(2+L)!}{2(L!)}$ is the number of the unique coefficients in an L^{th}-order Cartesian tensor. In the case of 4^{th}-order CT-ODFs, the multiplication $\mathbf{Cx}$ gives the 15 unique coefficients of a positive-definite tensor.

We applied our proposed method for estimating 4^{th}-order CT-ODFs ($L = 4$), using a set of $M = 321$ polynomial coefficients $\mathbf{c}_j$ and $\delta = 200$. Regarding the parameter δ, we performed several experiments using different values $\delta > 100$ and we obtained similar fiber orientations density profiles, which shows that our method is not sensitive to the selection of the value of δ.

2.3 Computing CT-ODF from Higher-Order Diffusion Tensor

Now, we present an application of our proposed framework for computing the coefficients of a CT-ODF from a given higher-order diffusion tensor and diffusion weighting b-value b, which is an essential task since the maxima of higher-order tensors do not correspond to the underlying fiber orientations. Given a higher-order diffusion tensor, the coefficients of the corresponding CT-ODF are computed by using the technique we presented in the previous section as follows

$$\mathbf{CB}^{-1} exp(-b\mathbf{Gt}) \tag{7}$$

where the matrices $\mathbf{C}$ and $\mathbf{B}$ are as defined in the previous section, $\mathbf{G}$ is of size $N \times \frac{(2+L)!}{2(L!)}$ and contains only monomials constructed from N unit vectors $\mathbf{g}_i$ uniformly distributed on the unit sphere, and $\mathbf{t}$ is a vector of size $\frac{(2+L)!}{2(L!)}$ that contains the unique coefficients of the given higher-order diffusion tensor. For example, in the case of 4^{th}-order tensors, the 15 unique coefficients are given in the vector $\mathbf{t}$, and $\mathbf{G}$ is of size $N \times 15$.

Note that in Eq. 7 the exponential function $exp()$ acts in an element-by-element fashion. Furthermore, the matrix inversion in Eq. 7 should be performed using non-negative least squares, as it has been shown in the previous section.

3 Experimental Results

In this section, we present experimental results of the proposed method applied to simulated as well as real DW-MRI data from a post-mortem porcine brain.

3.1 Synthetic Dataset

The proposed method was tested on a synthetic dataset by comparing the actual fiber orientations with the maxima of estimated CT-ODFs. In order to compare our results with spherical deconvolution techniques, included is also the results obtained using MOW [15], QBI [3], DOT [5] and MOVMF [16] methods by computing the maxima of either the PDF or ODF profiles of the corresponding methods.

The data was generated by simulating the MR signal from two crossing fibers whose orientations are $(cos20^\circ,\ sin20^\circ,\ 0)$ and $(cos100^\circ,\ sin100^\circ,\ 0)$ using the realistic diffusion MR simulation model in [17] with $b\text{-}value = 1500s/mm^2$ and 81 gradient directions. Six distinct Rician noise levels were added to the simulated data and for each noise level the experiments were repeated 100 times.

Figure 1 shows a plot of the means and standard deviations of deviation angles between the actual fiber orientations and the maxima of estimated CT-ODFs. For the particular noise level with std. dev. = 0.08 the deviation angles for all the methods are reported in the adjacent table. Also notice that in this experiment the deviation angle of the computed orientations is compared to its closest actual fiber orientation because the crossing fibers are weighted equally in generating the MR signals. The results demonstrate the superiority of the proposed method over QBI, DOT, MOVMF and MOW methods.

3.2 Real Dataset

Here we present CT-ODFs computed from high-quality DWI on post-mortem pig brain, which resemble the human brain in neuroanatomical complexity and

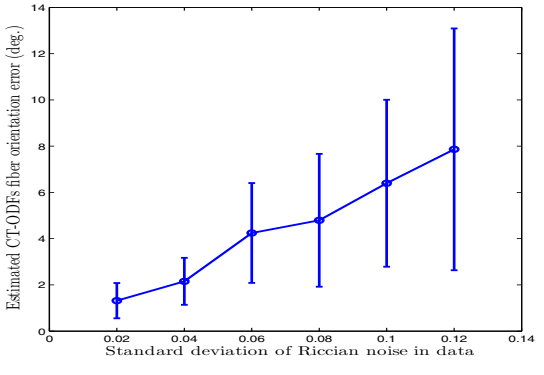

Table of errors (deg.)
noise st. dev. = 0.08

Method	Mean	St. dev.
QBI	9.125	±4.545
DOT	6.645	±3.720
MOVMF	5.624	±3.514
MOW	5.010	±2.955
CT-ODF	4.7926	±2.8726

Fig. 1. Deviation angle between actual fiber orientations and maxima of estimated CT-ODFs using a simulated 2-fiber crossing data with orientations $(cos20^\circ,\ sin20^\circ,\ 0)$ and $(cos100^\circ,\ sin100^\circ,\ 0)$ at different levels of Rician noise

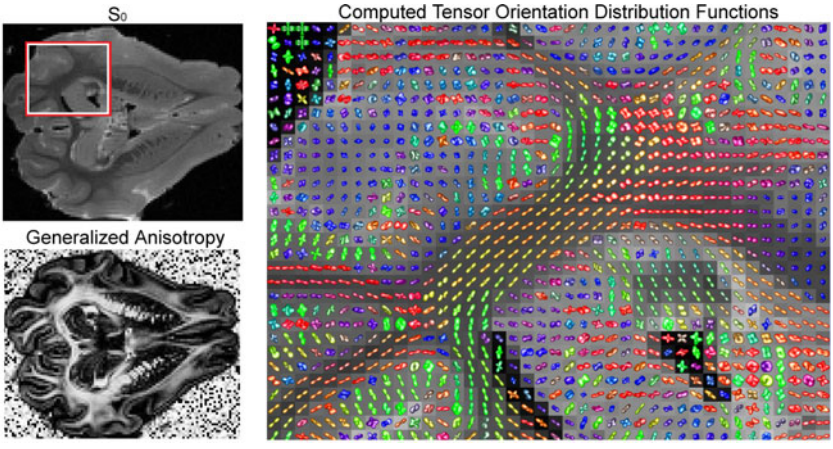

Fig. 2. CT-ODF field estimated by the proposed technique using data from a post-mortem porcine brain

where perfusion fixation was used to ensure that tissue characteristics were comparable to in vivo conditions [18]. Images are acquired using a pulsed gradient spin echo pulse sequence with echo time of $60ms$, 128×128 matrix with 10 slices, and voxel size of $0.5 \times 0.5 \times 0.5mm^3$. Three image were collected without diffusion weighting ($b \sim 0s/mm^2$) and 61 DWI with gradient strength $61mT/m$, gradient duration $23ms$, and gradient separation $30ms$. Each of these image sets used different diffusion gradients with approximate b values of $3146s/mm^2$. Fig. 2 shows CT-ODFs computed using our method along with generalized anisotropy and S_0 images. As can be verified in the generalized anisotropy image; the branching, bending and crossing of white matter tracts are correctly depicted by the computed CT-ODFs.

4 Conclusions

We presented a novel technique to estimate ODFs modeled as SPD high order tensors from DW-MR images. The performance of the proposed method is compared against several existing ODF measures on a synthetic dataset with different noise levels and outperformed the other methods. We also demonstrated the use of our method on a real DT-MR image obtained from a post-mortem porcine brain. Our results clearly demonstrate that crossing and merging of fibers are correctly depicted with CT-ODFs. Since higher order tensors have been used for segmentation, registration and computations of anisotropy measures for DT images, it remains to be seen if these tasks can be performed with the proposed CT-ODF fields as well.

References

1. Tuch, D., Weisskoff, R., Belliveau, J., Wedeen, V.J.: High angular resolution diffusion imaging of the human brain. In: ISMRM, p. 321 (1999)
2. Alexander, D., Barker, G., Arridge, S.: Detection and modeling of non-Gaussian apparent diffusion coefficient profiles in human brain data. MRM 48(2), 331–340 (2002)
3. Tuch, D.: Q-ball imaging. MRM 52(6), 1358–1372 (2004)
4. Wedeen, V., Hagmann, P., Tseng, W., Reese, T., Weisskoff, R.: Mapping complex tissue architecture with diffusion spectrum magnetic resonance imaging. MRM 54(6), 1377–1386 (2005)
5. Özarslan, E., Shepherd, T., Vemuri, B., Blackband, S., Mareci, T.: Resolution of complex tissue microarchitecture using the diffusion orientation transform (DOT). NeuroImage 31(3), 1086–1103 (2006)
6. Ozarslan, E., Mareci, T.: Generalized diffusion tensor imaging and analytical relationships between diffusion tensor imaging and high angular resolution diffusion imaging. MRM 50(5), 955–965 (2003)
7. Barmpoutis, A., Hwang, M., Howland, D., Forder, J., Vemuri, B.: Regularized positive-definite fourth order tensor field estimation from DW-MRI. Neuroimage 45(1S1), 153–162 (2009)
8. Ghosh, A., Deriche, R., Moakher, M.: Ternary quartic approach for positive 4th order diffusion tensors revisited. In: ISBI, pp. 618–621 (2009)
9. Barmpoutis, A., Vemuri, B.C.: A unified framework for estimating diffusion tensors of any order with symmetric positive-definite constraints. In: ISBI, pp. 1385–1388 (2010)
10. Yassine, I., McGraw, T.: 4th order diffusion tensor interpolation with divergence and curl constrained Bézier patches. In: ISBI, pp. 634–637 (2009)
11. Bloy, L., Verma, R.: On computing the underlying fiber directions from the diffusion orientation distribution function. In: Metaxas, D., Axel, L., Fichtinger, G., Székely, G. (eds.) MICCAI 2008, Part I. LNCS, vol. 5241, p. 8. Springer, Heidelberg (2008)
12. Schultz, T., Seidel, H.: Estimating crossing fibers: A tensor decomposition approach. TVCG 14(6), 1635–1642 (2008)
13. Zhan, W., Stein, E., Yang, Y.: Mapping the orientation of intravoxel crossing fibers based on the phase information of diffusion circular spectrum. NeuroImage 23(4), 1358–1369 (2004)
14. Von dem Hagen, E., Henkelman, R.: Orientational diffusion reflects fiber structure within a voxel. MRM 48(3), 454–459 (2002)
15. Jian, B., Vemuri, B., Özarslan, E., Carney, P., Mareci, T.: A novel tensor distribution model for the diffusion-weighted MR signal. NeuroImage 37(1), 164–176 (2007)
16. Kumar, R., Barmpoutis, A., Vemuri, B., Carney, P., Mareci, T.: Multi-fiber reconstruction from DW-MRI using a continuous mixture of von Mises-Fisher distributions. In: CVPR Workshop, pp. 1–8 (2008)
17. Söderman, O., Jönsson, B.: Restricted diffusion in cylindrical geometry. JMR, Series A 117(1), 94–97 (1995)
18. Dyrby, T., Baaré, W., Alexander, D., Jelsing, J., Garde, E., Søgaard, L.: An ex vivo imaging pipeline for producing high-quality and high-resolution diffusion-weighted imaging datasets. In: HBM (2010)